Opposite deformations between protons and neutrons in proton-rich C isotopes

Y. Kanada-En'yo*
Yukawa Institute for Theoretical Physics, Kyoto University, Kyoto 606-01, Japan

H. Horiuchi
Department of Physics, Kyoto University, Kyoto 606-01, Japan
(Received 12 November 1996)

Structures of C isotopes from the proton drip line to the neutron drip line are investigated in the framework of the antisymmetrized molecular dynamics (AMD). In particular, opposite deformations between protons and neutrons near the proton drip line are discussed in detail. We make certain of this new phenomenon suggested in the AMD results by analyzing the ratios of electric moments or transitions [Q or $B(E2)$] in ^{10}C and ^{11}C to those in the mirror nuclei ^{10}Be and ^{11}B. [S0556-2813(97)02206-1]

PACS number(s): 21.60.−n, 02.70.Ns, 21.10.Ky, 27.20.+n

I. INTRODUCTION

Unstable nuclei are expected to exhibit new phenomena which are not familiar in the stable nucleus region. Some properties of unstable nuclei are concerned with differences between proton and neutron densities, for instance the neutron halo and the neutron skin structure. Another problem of great interest is the difference between proton and neutron deformations. In this paper we suggest an opposite deformation between protons and neutrons in proton-rich C isotopes based on calculations within the framework of the antisymmetrized molecular dynamics (AMD) [1–4]. While we usually know proton densities by the data of electric properties, there are few data that tell us about neutron densities. Therefore we get the information on neutron densities from the data of electric properties of the mirror nuclei assuming mirror symmetry.

AMD has been already proved to be a very useful theoretical approach for investigations on nuclear structures in the light unstable nucleus region as well as the stable nucleus region. In the previous works on Li, Be, and B isotopes [2,3], it has been found that the intrinsic deformations of proton and neutron density distributions change rapidly as a function of the neutron and proton numbers. The experimental data of electric and magnetic properties of these unstable nuclei have been well reproduced without effective charges and g factors, but using only bare charges and g factors. This success is due to the flexible nature of the AMD wave function which can describe drastic changes of proton and neutron structures without any model assumptions such as the existence of clusters and axial symmetry.

The purpose of this paper is to investigate structures of C isotopes focusing on the deformations of protons and neutrons with the AMD method. We try to confirm a suggested problem of the opposite deformations between protons and neutrons by the help of the experimental data of electric moments and transitions in C and those in the mirror nuclei.

In Sec. II, the formulation of the AMD is briefly explained. In Sec. III, results of calculations with the AMD for C isotopes are displayed and compared to the experimental data. Discussions of the intrinsic deformations are presented in Sec. IV. The proton deformations and the neutron deformations of the isotopes are analyzed as a function of the neutron number N. Opposite deformations between the protons and the neutrons are found in the proton-rich C isotopes. A detailed discussion of deformations in ^{11}C and ^{10}C is presented by analyzing the electric quadrupole moments and $E2$ transitions, respectively. Finally, in Sec. V, a summary is given.

II. FORMULATION OF AMD AND ADOPTED FORCE

Here we give a brief explanation of the AMD framework. For a more detailed explanation the reader is referred to Refs. [1,2].

In the AMD the wave function of the A-nucleon system is written by a parity-projected Slater determinant:

$$|\Phi^{\pm}(\mathbf{Z})\rangle=(1\pm P)\frac{1}{\sqrt{A!}}\det[\varphi_i(j)],\quad \varphi_i=\phi_{\mathbf{Z}_i}\chi_{\alpha_i}, \quad (1)$$

where χ_{α_i} is a spin isospin function and $\phi_{\mathbf{Z}_i}$ is a spatial wave function with Gaussian form:

$$\langle\mathbf{r}|\phi_{\mathbf{Z}_i}\rangle=\left(\frac{2\nu}{\pi}\right)^{3/4}\exp\left[-\nu\left(\mathbf{r}-\frac{\mathbf{Z}_i}{\sqrt{\nu}}\right)^2+\frac{1}{2}\mathbf{Z}_i^2\right]. \quad (2)$$

In order to construct the ground state, we make an energy variational calculation for the trial function $\Phi^{\pm}(\mathbf{Z})$ by introducing the frictional cooling equations to the complex parameters $\{\mathbf{Z}\}$ as follows:

$$\dot{\mathbf{Z}}_j=(\lambda+i\mu)\frac{1}{i\hbar}\frac{\partial}{\partial\mathbf{Z}_j^*}\frac{\langle\Phi^{\pm}(\mathbf{Z})|H|\Phi^{\pm}(\mathbf{Z})\rangle}{\langle\Phi^{\pm}(\mathbf{Z})|\Phi^{\pm}(\mathbf{Z})\rangle}, \quad \text{c.c.}, \quad (3)$$

with arbitrary real numbers λ and $\mu<0$. It is easily proved that the energy of the system decreases with time:

*Present address: Institute of Particle and Nuclear Studies, 3-2-1 Midori-cho, Tanashi, Tokyo 188, Japan.

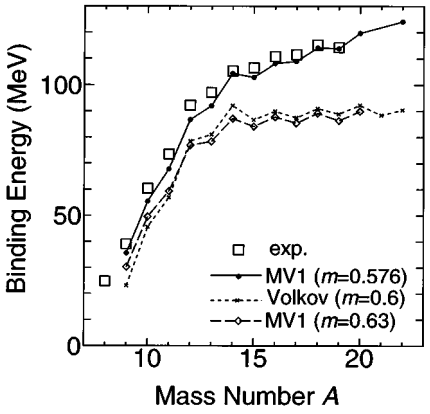

FIG. 1. Binding energies of C isotopes. The lines are AMD calculations with the MV1 force and the Volkov No. 1 force.

$$\frac{d}{dt}\frac{\langle\Phi^{\pm}(\mathbf{Z})|H|\Phi^{\pm}(\mathbf{Z})\rangle}{\langle\Phi^{\pm}(\mathbf{Z})|\Phi^{\pm}(\mathbf{Z})\rangle}<0. \tag{4}$$

We regard the energy minimum $|\Phi^{\pm}(\mathbf{Z})\rangle$ obtained after a long enough cooling time as the intrinsic state. Then the intrinsic state is projected on total angular momentum eigenstates $|P^{J}_{MK}\Phi^{\pm}(\mathbf{Z})\rangle$ with numerical integration. For each spin J, a K quantum number is chosen so as to make the projected energy minimum. Only in calculations of energy levels do we perform diagonalization of the Hamiltonian matrix with respect to the K quantum number, which shows that in the usual case K mixing is small and energies of the lowest levels hardly change with K mixing. The optimum width parameter ν of the Gaussian wave packets is determined for each parity state of each nucleus so as to get the minimum energy.

The adopted interaction in the present calculations of C isotopes is almost the same as that in Ref. [3] on B isotopes. The interaction is composed of the Volkov No. 1 force [5] as the two-body central force, the G3RS force with $u=u_I=-u_{II}=900$ MeV as the two-body LS force [7], the density-dependent force [6], and the Coulomb force. The strength of the repulsive part of the Volkov No. 1 force is weakened because of the use of the repulsive density-dependent force [6]. The modified Volkov No. 1 force together with the density-dependent force of Ref. [6] is called the MV1 force [6].

III. BINDING ENERGIES AND ELECTRIC PROPERTIES

Before treating our main subject, the study of the deformation of C isotopes, we first give some results which demonstrate the reliability of obtained AMD wave functions of C isotopes. Namely we show that the AMD can reproduce well the data of binding energies and electric properties of C isotopes. In Fig. 1 we compare the experimental binding energies with theoretical values calculated with MV1 force with the Majorana exchange mixture $m=0.576$ and $m=0.63$ and also with those calculated with Volkov No. 1 force with $m=0.60$. We see that the MV1 force with $m=0.576$ gives us a good fitting to the data over the whole C isotope. The theoretical energy for ^{15}C is the one for the $5/2^{+}$ state which is the lowest level in the present calculation. Electric quadrupole moments and $E2$ transition strengths are compared between theory and experiments in Figs. 2 and 3, respectively. Here the comparisons are made for C isotopes and their mirror nuclei and also for a neighboring nucleus ^{9}Be. The experimental data are seen to be well reproduced without any effective charges, but with bare charges.

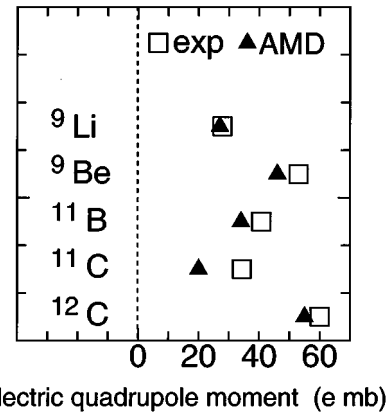

FIG. 2. Electric quadrupole moments of ground states of light nuclei. Only the ^{12}C, Q moment of the first 2^{+} state is displayed. Results with MV1 force ($m=0.576$) are compared with the experimental data.

IV. DEFORMATIONS OF PROTON AND NEUTRON DISTRIBUTIONS

A. Intrinsic deformations

In order to discuss intrinsic deformations of the proton and the neutron density distributions in C isotopes, we display in Fig. 4 the deformation parameters (β,γ) defined by the moments $\langle x^2\rangle$, $\langle y^2\rangle$, and $\langle z^2\rangle$ of the intrinsic AMD states as

$$\frac{\langle x^2\rangle^{1/2}}{(\langle x^2\rangle\langle y^2\rangle\langle z^2\rangle)^{1/6}}\equiv\exp(\delta_1)=\exp\left[\sqrt{\frac{5}{4\pi}}\beta\cos\left(\gamma+\frac{2\pi}{3}\right)\right], \tag{5}$$

$$\frac{\langle y^2\rangle^{1/2}}{(\langle x^2\rangle\langle y^2\rangle\langle z^2\rangle)^{1/6}}\equiv\exp(\delta_2)=\exp\left[\sqrt{\frac{5}{4\pi}}\beta\cos\left(\gamma-\frac{2\pi}{3}\right)\right],$$

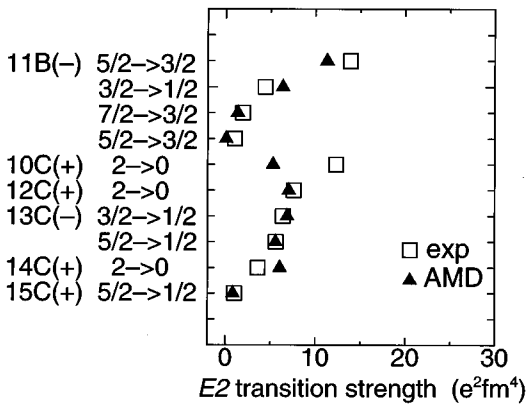

FIG. 3. $E2$ transition strength calculated with MV1 ($m=0.576$) are displayed with the experimental data.

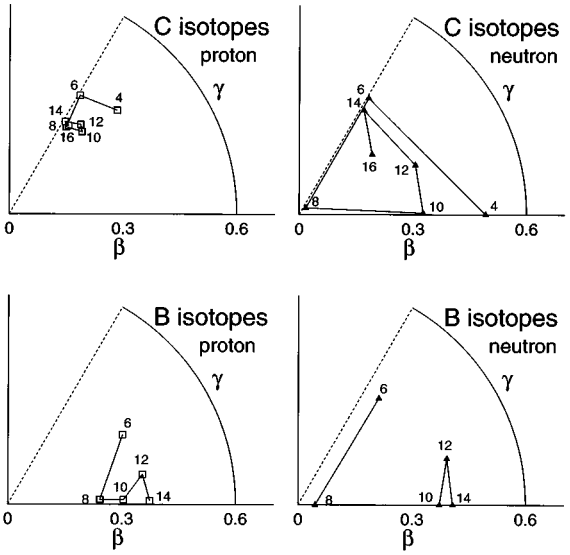

FIG. 4. Deformation parameters (β,γ) of the intrinsic states of AMD for B and C isotopes. Squares and triangles indicate (β,γ) for proton and neutron densities, respectively. Calculations are with the MV1 force. The neutron number N is written beside each point in the figures.

$$\frac{\langle z^2\rangle^{1/2}}{(\langle x^2\rangle\langle y^2\rangle\langle z^2\rangle)^{1/6}} \equiv \exp(\delta_3) = \exp\left[\sqrt{\frac{5}{4\pi}}\beta\cos\gamma\right].$$

Here the x, y, and z directions are chosen so as to satisfy $\langle x^2\rangle \leqslant \langle y^2\rangle \leqslant \langle z^2\rangle$. Results shown in Fig. 4 are those calculated with Majorana parameter $m=0.576$ for C nuclei. In case of Majorana parameters $m=0.60$ and 0.63, the behavior of the deformation parameters is very similar to the results with $m=0.576$. We also display deformation parameters for B isotopes of AMD calculations with mass-dependent Majorana parameters which were already found to reproduce the radii and Q moments of B isotopes in the previous paper [3]. We see in Fig. 4 the drastic change of the neutron deformation parameters ($\beta=\beta_n$, $\gamma=\gamma_n$) as a function of the neutron number N. Neutron deformations vary as prolate, oblate, spherical, prolate, and oblate as N increases from 4 to 16. On the other hand, the deformation parameters (β_p,γ_p) for the proton density remain in a compact region near the oblate line for all C isotopes in spite of the variety of neutron deformation as a function of neutron number N. The stability of the proton deformation is a unique point of C isotopes in contrast to the situation in Li, Be, and B isotopes which, according to AMD calculations, have β or γ soft proton densities. In the case of B isotopes with $Z=5$ the proton shape changes as N increases by the influence of the mean field given by the deformed neutron density [3]. On the other hand, the proton deformation in C isotopes is oblate and invariable for any neutron numbers.

It is notable that in proton-rich C nuclei neutrons whose number is less than 6 ($3\leqslant N\leqslant 5$) prefer prolate or triaxial deformations rather than oblate shape. As a result, a disagreement between the proton and the neutron deformations is found in proton-rich C isotopes. The detailed behavior of deformation parameters of proton-rich C isotopes is illustrated in Fig. 5. Squares and triangles correspond to (β,γ) for proton and neutron deformations, respectively. In the following subsections we study in detail the opposite shapes between the protons and the neutrons in ^{11}C and ^{10}C.

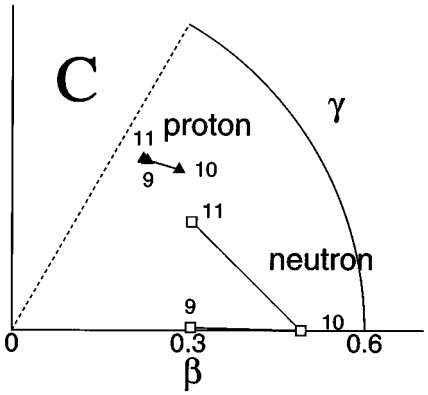

FIG. 5. Deformation parameters (β,γ) for proton and neutron densities in the intrinsic states of proton-rich C isotopes with $A=9-11$ are given by triangles and squares, respectively. The mass number A is indicated beside each point in the figure.

B. Deformations in ^{11}C

Our purpose here is to confirm the disagreement of the proton and the neutron deformations in proton-rich C isotopes by the help of the electric quadrupole moments and transitions in C and in the mirror nuclei. First we discuss Q moments of ^{11}C and the mirror nucleus ^{11}B. From the data of the electric Q moment of ^{11}C we get information on the intrinsic deformation of the proton density of ^{11}C while we can get information on the neutron deformation of ^{11}C from the data of the electric Q moment of the mirror nuclei ^{11}B under the assumption of mirror symmetry. According to the experimental data, Q moment of ^{11}B with $Z=5$ is larger than that of ^{11}C with $Z=6$, which seems to be inconsistent with the charges of these nuclei. The seeming inconsistency in the Q moments of ^{11}C and ^{11}B can be explained with the difference between proton and neutron deformations in ^{11}C. In other words, the opposite deformations of protons and neutrons are reflected by the electric moments of the mirror nuclei ^{11}C and ^{11}B and are consistent with the experimental data.

Based on mirror symmetry for proton and neutron deformations, we compare below quantitatively the proton and neutron deformations by analyzing the ratio of the electric quadrupole moment Q in ^{11}C to that in the mirror nucleus ^{11}B. We introduce the well-known approximate relation between the electric quadrupole moment Q in the laboratory frame and the intrinsic quadrupole moment Q_0:

$$Q = Q_0\frac{3K^2-J(J+1)}{(2J+3)(J+1)}. \tag{6}$$

By using Eq. (5) we can express the intrinsic electric quadrupole moment Q_0 as follows in the first order of the deformation parameter β_p:

$$Q_0 = \sqrt{\frac{16\pi}{5}}\frac{3}{4\pi}Ze\beta_p\cos\gamma_p R_e^2, \tag{7}$$

where β_p and γ_p are the deformation parameters for the proton density, and Z and R_e are the proton number and the

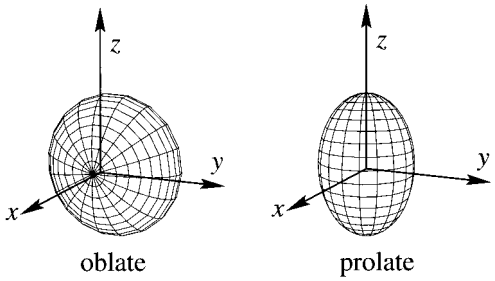

FIG. 6. Schematic figures of the nucleus with oblate proton and prolate neutron deformations. In the body-fixed flame x,y,z is chosen so that moments of inertia obey the relation $\mathcal{I}_{zz} \leqslant \mathcal{I}_{yy} \leqslant \mathcal{I}_{xx}$.

charge radius, respectively. Equation (7) has a form which is obtained by replacing the deformation parameter β_p in the usual equation $Q_0 = \sqrt{16\pi/5}(3/4\pi)Ze\beta_p R_e^2$ with an effective deformation parameter $\beta_p \cos\gamma_p$ for protons. We need to explain the appropriate principal axes in the nucleus where there coexist different proton and neutron shapes as shown in Fig. 6. For example in the nucleus with oblate proton and prolate neutron deformations, the approximate symmetry axis x for protons usually differs from the approximate symmetry axis z for neutrons so as to make the proton density overlap largely with the neutron density. In many cases, a symmetry axis z for the prolate neutron density is better to choose as the principal axis Z in the total intrinsic system for the total-angular momentum projection. In such cases, the usual formula for Q_0 is modified by using the effective deformation to the z axis $\beta_p \cos\gamma_p$ instead of β_p. In other words, an oblate deformation gives a smaller contribution to the intrinsic quadrupole moment with the principal axis chosen so as to have the minimum moment of inertia.

Assuming these simple approximations the ratio of the Q moment in ^{11}C to that in ^{11}B is represented by the product of three terms, the ratios of proton numbers, proton deformation parameters, and charge radii. When we assume the mirror symmetry for the deformation parameters and replace the deformation parameter $\beta_p \cos\gamma_p(^{11}\mathrm{B})$ for the proton density in ^{11}B by $\beta_n \cos\gamma_n(^{11}\mathrm{C})$ for the neutron density in ^{11}C, the ratio of Q is written as

$$\frac{Q(^{11}\mathrm{C})}{Q(^{11}\mathrm{B})} = \left(\frac{Z=6}{Z=5}\right) \times \left(\frac{\beta_p \cos\gamma_p(^{11}\mathrm{C})}{\beta_n \cos\gamma_n(^{11}\mathrm{C})}\right) \times \left(\frac{R_e(^{11}\mathrm{C})}{R_e(^{11}\mathrm{B})}\right)^2 . \quad (8)$$

We take the third term of charge radii to be unity since ^{11}C and ^{11}B are the nuclei close to the stability line. If the neutron deformation agrees with the proton deformation in ^{11}C as has been often considered, the second term gives no contribution to the ratio of Q moments and the ratio can be explained only by the charge ratio 1.2. However, the experimental data of $Q(^{11}\mathrm{C})$ is smaller than $Q(^{11}\mathrm{B})$; $Q(^{11}\mathrm{C})$ is 34.8 e mb and $Q(^{11}\mathrm{B})$ is 40.7 e mb. The ratio 0.88 deduced from the experimental data is less than a unity and is inconsistent with the Z ratio. According to AMD calculations, this problem can be resolved by taking into account the difference between the intrinsic deformations of proton and neutron densities in ^{11}C. Through the second term in Eq. (8), the ratio of Q moments reflects the difference of intrinsic shapes between proton and neutron densities. As shown above in Fig. 5 the proton deformation is oblate while the neutron density becomes triaxial in shape in ^{11}C. Since $\beta_p \cos\gamma_p(^{11}\mathrm{C})$ is smaller than $\beta_n \cos\gamma_n(^{11}\mathrm{C})$, the second term in Eq. (8) becomes less than unity, which cancels the effect of the first term of the Z ratio.

It should be pointed out that if the third term of charge radii in Eq. (8) is taken into account our argument is even more strongly supported. It is natural to expect that the ratio of charge radii $R_e^2(^{11}\mathrm{C})/R_e^2(^{11}\mathrm{B})$ is larger than unity. Then the experimental ratio 0.88 of Q moments is inconsistent with not only the first term of charge ratio but also the third term of squared charge radius ratio in Eq. (8) both of which are larger than unity. This inconsistency should be resolved by the second term. Namely a difference between proton and neutron shapes should be existent in ^{11}C in such a way that $\beta_p \cos\gamma_p < \beta_n \cos\gamma_n$.

We proceed with further quantitative discussion of the theoretical values of deformation parameters in the intrinsic states obtained with AMD. In the present results, the ground state of ^{11}C with $J=3/2$ is obtained by a total-angular-momentum projection on a state $|J=3/2, K=3/2\rangle$ with respects to the principal z axis chosen so as to make the moment of inertia minimum. Using the theoretical values of $\beta\cos\gamma$ shown in Fig. 5 we can estimate the ratio of Q moments with the first and the second terms in Eq. (8). The estimated ratio is found to be 0.87 which is as small as the value of 0.88 deduced from the experimental data. In fact the theoretical results of electric Q moments for total-angular momentum projected states are 20 e mb for ^{11}C and 34 e mb for ^{11}B, which are consistent with the data of $Q(^{11}\mathrm{C}) < Q(^{11}\mathrm{B})$ (Table I).

It is concluded that the difference in the intrinsic deformation of the proton density in ^{11}C from that in ^{11}B (an oblate shape in ^{11}C and a triaxial shape in ^{11}B) significantly effects the ratio of a Q moment in ^{11}C to that in ^{11}B. With the help of mirror symmetry, the theoretical suggestion of a disagreement between proton and neutron deformations in ^{11}C is supported by the experimental fact that the ratio of electric Q moments of ^{11}C to ^{11}B is less than unity.

C. Deformations in ^{10}C

We make a similar analysis of deformations for ^{10}C. We find that the difference between proton and neutron deformations in ^{10}C is important in order to understand the ratio of the electric quadrupole transition strength $B(E2;2^+ \rightarrow 0^+)$ in ^{10}C to that in the mirror nucleus ^{10}Be. Assuming a mirror symmetry similar to Eq. (8), the ratio of $B(E2)$ is approximated as

$$\frac{B(E2;^{10}\mathrm{C})}{B(E2;^{10}\mathrm{Be})} = \left(\frac{Z=6}{Z=4}\right)^2 \times \left(\frac{\beta_p \cos\gamma_p(^{10}\mathrm{C})}{\beta_n \cos\gamma_n(^{10}\mathrm{C})}\right)^2 \times \left(\frac{R_e(^{10}\mathrm{C})}{R_e(^{10}\mathrm{Be})}\right)^4 . \quad (9)$$

The first term of charge ratio $(6/4)^2 = 2.25$ is much larger than the ratio of experimental values $12.3(2.0)\ e^2\,\mathrm{fm}^4 / 10.5(1.0)\ e^2\,\mathrm{fm}^4 = 1.2(0.3)$. The reason why the square of the charge ratio fails to reproduce the ratio of $B(E2)$ in the mirror nuclei ^{10}C and ^{10}Be is because of the disagreement between proton and neutron deformations in ^{10}C.

In the intrinsic state of ^{10}C, the proton density deforms oblately with $\beta_p \cos\gamma_p = 0.28$ while the neutron deformation

TABLE I. Electric quadrupole moments and transitions of proton-rich C isotopes and the mirror nuclei. Calculations are with MV1 force ($m=0.576$) and the experimental data are taken from [8].

		Electric Q moments	
Nucleus	Level	exp.	theory
^{11}C	$3/2^-$	34.3 e mb	20 e mb
^{11}B	$3/2^-$	40.7(3) e mb	34 e mb
^{10}C	2^+		-38 e mb
^{10}Be	2^+		-65 e mb
^{9}C	$3/2^-$		-28 e mb
^{9}Li	$3/2^-$	-27.8 e mb	-27 e mb
		$E2$ transition strength	
nucleus	level	exp.	theory
^{11}C	$5/2^-\rightarrow 3/2^-$		6.8 e^2 fm^4
^{11}B	$5/2^-\rightarrow 3/2^-$	13.9(3.4) e^2 fm^4	11.3 e^2 fm^4
^{10}C	$2^+\rightarrow 0^+$	12.3(2.0) e^2 fm^4	5.3 e^2 fm^4
^{10}Be	$2^+\rightarrow 0^+$	10.5(1.0) e^2 fm^4	9.5 e^2 fm^4
^{9}C	$1/2^-\rightarrow 3/2^-$		5.7 e^2 fm^4
^{9}Li	$1/2^-\rightarrow 3/2^-$		7.2 e^2 fm^4

is prolate with a larger value of the effective deformation parameter $\beta_n\cos\gamma_n=0.49$ (Fig. 5), which makes the second term in Eq. (9) less than unity. Thus the ratio is roughly estimated as

$$\frac{B(E2;^{10}\mathrm{C})}{B(E2;^{10}\mathrm{Be})}=2.25\times(0.28/0.49)^2\sim 0.75. \qquad (10)$$

The reason for a smaller theoretical value of the ratio than the experimental one is considered to be due to the omission of the third term from the charge radius ratio in Eq. (9). Since ^{10}C is a nucleus near the proton dripline, effects of the charge radii are expected to be also significant and should be taken into consideration as well as the ratio of deformation parameters. It is to be noted that though the density tail of the proton is suppressed by the Coulomb barrier, the charge radii may give effects since $B(E2)$ is affected by charge radii to the forth power. We think it natural to consider that the third term in Eq. (9) may become larger than unity because the charge radius in proton-rich ^{10}C can be expected to be larger than that in ^{10}Be. We should point out that the consideration of the charge radius ratio [the third term of Eq. (9)] strongly supports our argument that a difference between proton and neutron shapes should be concluded in ^{10}C in order to explain the observed reduced value of the ratio $B(E2;^{10}\mathrm{C})/B(E2;^{10}\mathrm{Be})$.

The theoretical results with AMD calculations are shown in Table I and are compared with the experimental data. The calculations underestimate the value of $B(E2;^{10}\mathrm{C})$, therefore, the ratio $B(E2;^{10}\mathrm{C})/B(E2;^{10}\mathrm{Be})$ is underestimated. This is probably because the AMD wave function does not describe the precise behavior of long tails of valence nucleons as mentioned in our previous paper [2] regarding halo structures of neutron-rich nuclei. A detailed analysis of the wave functions for valence protons is required.

In the above arguments we analyzed quadrupole moments of the protons and the neutrons in the ground state of ^{10}C by investigating deformation parameters β and γ. We analyze below quadrupole moments from another viewpoint by studying the angular momentum components of protons and neutrons contained in the intrinsic wave function of the AMD. Roughly speaking the AMD tells us that the ^{10}C nucleus consists of two α and two valence protons (Fig. 7). In order to analyze this AMD wave function we consider the shell model limit of the AMD wave function which is constructed by making the α-α and α-p distances small. In this shell model limit, the intrinsic state is roughly represented by a simple configuration with four neutrons in $(0,0,0)^2(0,0,1)^2$ and six protons in $(0,0,0)^2(0,0,1)^2(0,1,0)^2$ in terms of harmonic-oscillator orbits (n_x,n_y,n_z), where we choose the z axis as the axis with the minimum moment of inertia and the x axis as the axis with the maximum moment of inertia. It is to be noted that since the intrinsic spins of a pair of two nucleons in the same orbit almost couple off to the singlet 0, only the orbital angular momenta of the four protons and two neutrons in the outer major shell should be taken into consideration in the discussion of Q moments. The lowest state with spin $J=2$ in ^{10}C is found to be a state $|JK\rangle=|2,0\rangle$ projected on a total angular momentum eigen-

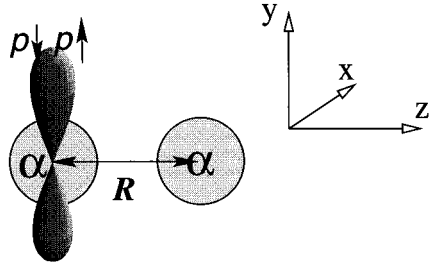

FIG. 7. A schematic figure for the intrinsic structure of ^{10}C calculated with AMD. ^{10}C approximately consists of 2α surrounded by $2p$ in a (0,1,0) orbit.

state with respect to the principal z axis. In the projected state $|2,0\rangle$ from the intrinsic state, the total spin $J=2$ mainly consists of the angular momentum of the relative coordinate **R** between α clusters (Fig. 7), while the angular momenta of the two protons in $(0,1,0)^2$ orbits which are equivalent to the linear combination of $|l,m\rangle=|1,\pm1\rangle$ contribute to $|JK\rangle=|2,\pm2\rangle$. Here $|l,m\rangle$ is a state in terms of the lm scheme with respect to the z axis in Fig. 7. It means that the two valence protons give no sizable contribution to the quadrupole moment of protons. Q moments are not as what is simply expected with the proton number. More strictly speaking, because of the occupation of $(0,1,0)^2_{p\uparrow p\downarrow}$ in the intrinsic system the Q moment of protons decreases in the total angular momentum projected state $|JK\rangle=|2,0\rangle$. A reduction mechanism of Q moment by protons in $(0,1,0)^2$ can be easily described by just the composition of the orbital angular momenta of four protons and two protons in the p shell. We consider a configuration in the shell model limit $(0,0,1)^2_{p\uparrow p\downarrow}$ $(0,1,0)^2_{p\uparrow p\downarrow}$ and $(0,0,1)^2_{n\uparrow n\downarrow}$. As to the orbital angular momenta of neutrons, two neutrons in orbits $(0,0,1)^2_{n\uparrow n\downarrow}$ construct total orbital angular momentum eigenstates for neutrons $|L_n,K_n\rangle=|0,0\rangle$ and $|2,0\rangle$ with the ratio 1:2 of amplitudes. In the case of the angular momenta of protons, an antisymmetrized state of $(0,0,1)^2_{p\uparrow p\downarrow}$ $(0,1,0)^2_{p\uparrow p\downarrow}$ which is the two-hole state $(1,0,0)^{-2}_{p\uparrow p\downarrow}$ constructs total orbital angular momentum eigenstates of protons $|L_p,K_p\rangle=|0,0\rangle$, $|2,0\rangle$, $|2,+2\rangle$, $|2,-2\rangle$ with the ratio $2:1:\frac{3}{2}:\frac{3}{2}$. Here one should note that the (1,0,0) state can be rewritten as $(1/\sqrt{2})(|1,1\rangle+|1,-1\rangle)$ by using the state $|l_p,m_p\rangle$ in the lm scheme. As far as states with $K=0$, the state $|L_p,K_p\rangle=|0,0\rangle$ is found to have a larger amplitude than the state $|2,0\rangle$ in the case of $(0,0,1)^2_{p\uparrow p\downarrow}$ $(0,1,0)^2_{p\uparrow p\downarrow}$. The reason is that the protons in single particle states $|l_p,m_p\rangle=|1,+1\rangle$ and $|1,-1\rangle$ which originate in $(0,1,0)^2_{p\uparrow p\downarrow}$ tend to couple their angular momenta so as to be totally $L_p=0$ rather than $L_p=2$ under a constraint of K quantum $K_p=0$. The point is that the neutrons in $(0,0,1)^2_{n\uparrow n\downarrow}$ construct the total orbital angular momentum $|L_nM_n\rangle=|0,0\rangle$ and $|2,0\rangle$ with the ratio 1:2, while in the case of the protons in $(0,0,1)^2(0,1,0)^2$ the amplitude of the state with $|L_pK_p\rangle=|0,0\rangle$ is larger than that of $|2,0\rangle$ with the ratio of 2:1. As a result, in the total system of protons and neutrons the total angular momentum projected state of $|JK\rangle=|2,0\rangle$ which consists mainly of $|L_n,M_n=2,0\rangle|L_p,M_p=0,0\rangle$ and $|L_n,M_n=0,0\rangle|L_p,M_p=2,0\rangle$ contains less components of the state with $L_p=2$ than the state with $L_n=2$. In fact, in the state $|2,0\rangle$ of ^{10}C obtained by AMD, the total orbital angular momentum of the protons is found to be rather smaller compared to that of the neutrons. Therefore we can say that the last two protons in a (0,1,0) orbital reduce the component with $L_p\neq0$ in $|2,0\rangle$ which results in a decrease of the Q moment of the proton density. This is quite consistent with the situation that $\langle y^2\rangle$ reduces Q moments in a system with an oblate deformation because we know that protons in the (0,1,0) orbital enlarge the expectation value of $\langle y^2\rangle$ of the proton density and make an oblate shape of the total proton density, that is to say decreased Q moments of protons.

Of course we should remind the reader that the realistic wave function of ^{10}C is not explained by such a simple configuration in terms of the shell model limit but it must contain a rich variety of more complex configurations and components with higher angular momentum due to the existence of α clusters and valence protons, and also due to the spin-orbit force.

V. SUMMARY

In summary, C isotopes up to the proton drip line were studied with AMD. The intrinsic deformation of the protons in C isotopes is usually oblate while the neutron structure changes rapidly as a function of neutron number N. Thus, one of the interesting results is the opposite deformations between protons and neutrons in proton-rich C isotopes. These unfamiliar results suggested with AMD were confirmed by analyzing the ratios of electric quadrupole moments and transitions [Q and $B(E2)$] in ^{10}C and ^{11}C to those in the mirror nuclei ^{10}Be and ^{11}B. The significant effect of the difference of the proton and the neutron shapes to the ratios of electric quadrupole moments and transitions of the mirror nuclei was disclosed with the help of deformation parameters in the intrinsic states. Oblate proton deformations in proton-rich C isotopes were shown to decrease electric quadrupole moments and transitions [Q and $B(E2)$] compared with those of the mirror nuclei.

ACKNOWLEDGMENTS

The authors would like to thank Dr. A. Ono for many discussions and helpful technical advice on the numerical calculations. They are also thankful to Professor W. von Oertzen for helpful discussions and encouragement. The valuable comments of Professor I. Tanihata and other experimentalists are also gratefully acknowledged. The computational calculations in this work was financially supported by the Research Center for Nuclear Physics, Osaka University.

[1] Y. Kanada-En'yo and H. Horiuchi, Prog. Theor. Phys. **93**, 115 (1995).
[2] Y. Kanada-En'yo, A. Ono, and H. Horiuchi, Phys. Rev. C **52**, 628 (1995).
[3] Y. Kanada-En'yo and H. Horiuchi, Phys. Rev. C **52**, 647 (1995).
[4] Y. Kanada-En'yo and H. Horiuchi, Phys. Rev. C **54**, R468 (1996).
[5] A. B. Volkov, Nucl. Phys. **74**, 33 (1965).
[6] T. Ando, K. Ikeda, and A. Tohsaki, Prog. Theor. Phys. **64**, 1608 (1980).
[7] N. Yamaguchi, T. Kasahara, S. Nagata, and Y. Akaishi, Prog. Theor. Phys. **62**, 1018 (1979); R. Tamagaki, *ibid.* **39**, 91 (1968).
[8] P. Raghavan, At. Data Nucl. Data Tables **42**, 189 (1989).